European Journal of Control 86 (2025) 101375

Contents lists available at ScienceDirect

European Journal of Control

journal homepage: www.sciencedirect.com/journal/european-journal-of-control

# Output-feedback integrated fault-tolerant control for discrete-time systems subject to input and state constraints

Marcin Witczak [a], Damiano Rotondo [b,*], Marcin Pazera [a], Vicenç Puig [c]

[a] Institute of Control and Computation Engineering, University of Zielona Gora, ul. Szafrana 2, Zielona Gora, 65-516, Poland
[b] Department of Electrical and Computer Engineering (IDE), University of Stavanger, Kristine Bonnevies vei 22, Stavanger, 4021, Norway
[c] Institut de Robotica i Informatica Industrial (CSIC-UPC), Universitat Politecnica de Catalunya, Barcelona, 08034, Spain

ARTICLE INFO

Recommended by T. Parisini

*Keywords:*
Fault tolerant control
LMI
Fault estimation
Output feedback
Constrained control

ABSTRACT

The paper deals with the problem of integrated fault estimation and fault tolerant control for constrained linear systems with bounded external disturbances. In particular, the above coupling causes that control and estimation influence each other. Thus, to prevent an unacceptable performance of the entire system, a new integration strategy is proposed, The proposed framework is based on an output feedback framework that consists of two stages: *off-line* – a low-complexity LMI-based optimization task and *on-line* – a deterministic model predictive control problem. The proposed approach is assessed using a cascade two-tank system example.

## 1. Introduction

As demonstrated in many seminal works (see Lan and Patton (2021) and the references therein), fault estimation (FE) (Han, Liu, Wei and Zhu, 2023; Witczak, 2014; Witczak, Pazera, Majdzik, & Matysiak, 2024) and fault-tolerant control (FTC) (Kukurowski, Mrugalski, Pazera, & Witczak, 2022; Xiao, Liu, & An, 2024) play an important role in modern control theory and practice. A standard approach is to implement FE and FTC sequentially, that is, by designing each component separately; see, e.g., Han, Liu, Xie and Wei (2023). However, in this sequential approach, the effect of the fault estimator on the controller's performance can be addressed only through the selection of the controller gain. In contrast, an integrated strategy, where FE and FTC are designed simultaneously, enables the controller performance to be influenced not only by the controller gains but also through the appropriate selection of the fault estimator gains.

The concept of an output feedback-based simultaneous integrated FTC was introduced in Witczak, Dziekan, Puig, and Korbicz (2008) for linear and Takagi–Sugeno (T-S) deterministic systems. Subsequently, it was also adapted to linear parameter varying (LPV) and Lipschitz systems (Montes de Oca, Puig, Witczak, & Dziekan, 2012; Witczak, Puig, & de Oca, 2013). The integrated FTC was extended to linear non-deterministic systems in Lan and Patton (2016a). This work indicates also an undesired effect of bidirectional influence between FE and FTC. To address this challenging problem, the authors proposed both state and output feedback strategies by solving FE and FTC with a single linear matrix inequality (LMI)-based optimization task. The strategy was further adapted to Lipschitz (Hashemi & Tan, 2020), T-S (Lan & Patton, 2016b) as well as LPV (Do, Koenig, & Theilliol, 2020) systems. Irrespective of the incontestable appeal of the above approaches, they all inherit one common drawback pertaining to the complexity of the underlying LMIs. The problem becomes even worse when dealing with complex systems described using either LPV or T-S frameworks. To overcome these difficulties, the work (Lan & Patton, 2022) proposes an iterative solution, which aims at handling the above bidirectional interactions with a reduced complexity pertaining to the underlying LMIs. In spite of the incontestable appeal of the above approach, it does not take into account the input and output constraints of the considered system. This is particularly important for the cases when actuator faults appear in the system, and hence, the above constraints become time-varying.

The work in Rotondo, Pazera, and Witczak (2025) demonstrated that the interplay between control and estimation in systems with state and input constraints can be effectively managed using the concept of quadratic boundedness (Alessandri, Baglietto, & Battistelli, 2006). The proposed integration strategy results in an output-feedback FTC scheme comprising two stages:

1. An offline stage, which involves a low-complexity optimization problem based on LMIs.
2. An online stage, where a model predictive control problem is solved via quadratic programming.

* Corresponding author.
*E-mail address:* damiano.rotondo@uis.no (D. Rotondo).

https://doi.org/10.1016/j.ejcon.2025.101375
Received 13 February 2025; Received in revised form 31 July 2025; Accepted 31 August 2025
Available online 10 September 2025
0947-3580/© 2025 The Authors. Published by Elsevier Ltd on behalf of European Control Association. This is an open access article under the CC BY license (http://creativecommons.org/licenses/by/4.0/).

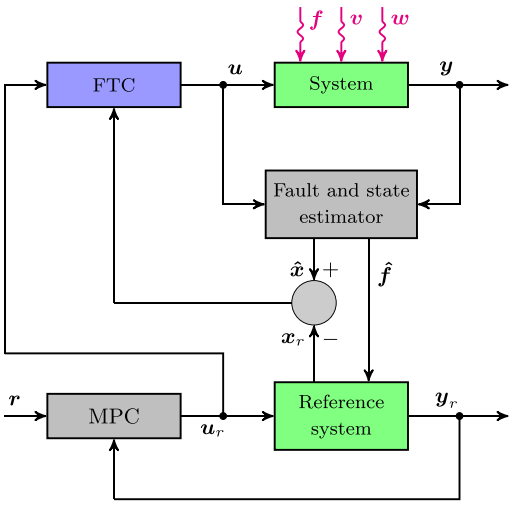


**Fig. 1.** The proposed output feedback FTC.

This framework, illustrated in Fig. 1, provides a robust approach to integrated FTC. In particular, FTC as well as state and fault estimators are designed during an offline stage, which pertains to solving a set of LMIs that result in appropriate gain matrices for the estimator and the controller. Subsequently, MPC pertains to the online stage and it is responsible for controlling the reference system.

While the continuous-time formulation in Rotondo et al. (2025) offers a strong theoretical foundation, its practical implementation is challenged by the digital nature of modern control platforms. Although continuous-time designs are common, they lack full theoretical rigour in digital settings, as they presume an ideal high sampling rate that may be impractical. Some approaches, such as the use of inter-sample predictors (Karafyllis, Ahmed-Ali, & Giri, 2020), attempt to address this gap by estimating the state evolution between sampling instants, but these often introduce significant complexity.

The present paper addresses these challenges by developing a discrete-time counterpart to the continuous-time integrated FTC framework proposed in Rotondo et al. (2025). Importantly, this extension is not a straightforward transposition, as it requires dedicated mathematical treatment to accommodate the structural differences of discrete-time dynamics. In particular, the discrete-time derivations rely on ad hoc reformulations that decouple the Lyapunov and system matrices, an essential step for casting the integrated design conditions into LMI form. This is crucial to ensure the resulting conditions are tractable and solvable using standard convex optimization tools. For clarity and focus, the focus of the paper is on time-invariant systems. However, the proposed framework can be readily extended to parameter-varying systems by exploiting polytopic representations and Polya's theorem on definite quadratic forms (Braga, Morais, Tognetti, Oliveira, & Peres, 2015; Sala & Ariño, 2007).

The main goal of this paper is to formulate a novel approach to the design of an integrated FTC for a class of linear systems with time-varying constraints. The primary contributions can be summarized as follows:

- Contrarily to the approaches presented in the literature (Lan & Patton, 2016a, 2021; Witczak, Buciakowski, & Aubrun, 2016), it is proposed that the deterministic reference system control strategy is designed with the knowledge about faults. This guarantees that the resulting reference output is the closest possible one to a given reference under fault conditions.
- The proposed output feedback FTC allows tracking of the reference system under time-varying input and state limitations.
- The developed approach consists of two stages: *off-line* involves resolving a low-complexity LMI-based optimization challenge, while the *on-line* stage involves resolving an MPC based on quadratic programming.

The paper is organized as follows. Section 2 recalls necessary definitions and lemmas as well as proposes the tools for settling the problem being stated. Section 3 presents the problem formulation. Section 4 describes the integrated design approach while Section 5 details the whole design procedure. Section 6 exhibits a numerical example concerning a cascade two-tank system. This example is used to illustrate the benefits and limitations associate with the proposed approach. Finally, Section 7 concludes the paper.

## 2. Preliminaries

The objective of this section is to provide technical tools, which will be employed for the FTC designed presented in the subsequent sections of this paper.

Let us consider the dynamic system:

$$\boldsymbol{z}_{k+1} = \boldsymbol{F}\boldsymbol{z}_k + \boldsymbol{G}\boldsymbol{d}_k \tag{1}$$

where $\boldsymbol{z}_k \in \mathbb{R}^{n_z}$ is the state and $\boldsymbol{d}_k \in \mathbb{D} \subset \mathbb{R}^{n_d}$ stands for the exogenous disturbance vector. Additionally, $\boldsymbol{F} \in \mathbb{R}^{n_z \times n_z}$, $\boldsymbol{G} \in \mathbb{R}^{n_z \times n_d}$. Moreover, let $\mathbb{E}_d = \{\boldsymbol{d}_k : \boldsymbol{d}_k^T \boldsymbol{Q}_d \boldsymbol{d}_k \leq 1\}$, $\boldsymbol{Q}_d \succ \boldsymbol{0}$ denote an ellipsoidal set. For the purpose of further deliberations, let us define the Lyapunov function $V_k = \boldsymbol{z}_k^T \boldsymbol{P} \boldsymbol{z}_k$, $\boldsymbol{P} \succ \boldsymbol{0}$ and the associated ellipsoidal set $\mathbb{E}_z = \{\boldsymbol{z}_k : \boldsymbol{z}_k^T \boldsymbol{P} \boldsymbol{z}_k \leq 1\}$.

**Definition 1** (*Alessandri et al., 2006*)**.** The system (1) is strictly quadratically bounded with $V_k$ if $V_k > 1$ implies $V_{k+1} - V_k < 0$ for all allowable $\boldsymbol{d}_k \in \mathbb{E}_d$.

**Definition 2** (*Alessandri et al., 2006*)**.** $\mathbb{E}_z$ is a positively invariant set for the system (1) if $\boldsymbol{z}_k \in \mathbb{E}_z$ implies $\boldsymbol{z}_{k+1} \in \mathbb{E}_z$ for all $\boldsymbol{d}_k \in \mathbb{E}_d$.

**Lemma 1** (*Alessandri et al., 2006*)**.** *The following statements are equivalent:*

1. *The system (1) is strictly quadratically bounded with $V_k$ for all $\boldsymbol{d}_k \in \mathbb{E}_d$.*
2. *The ellipsoid $\mathbb{E}_z$ is positively invariant for all $\boldsymbol{d}_k \in \mathbb{E}_d$.*
3. *There exists $\alpha \in (0,1)$ such that the following inequality is satisfied for all $\boldsymbol{d}_k \in \mathbb{E}_d$:*

$$V_{k+1} - (1-\alpha) V_k - \alpha \boldsymbol{d}_k^T \boldsymbol{Q}_d \boldsymbol{d}_k < 0 \tag{2}$$

4. *There exists $\alpha \in (0,1)$ such that (3) holds.*

$$\begin{bmatrix} \boldsymbol{F}^T \boldsymbol{P} \boldsymbol{F} + (\alpha - 1)\boldsymbol{P} & \boldsymbol{F}^T \boldsymbol{P} \boldsymbol{G} \\ \boldsymbol{G}^T \boldsymbol{P} \boldsymbol{F} & \boldsymbol{G}^T \boldsymbol{P} \boldsymbol{G} - \alpha \boldsymbol{Q}_d \end{bmatrix} \prec 0 \tag{3}$$

5. *There exists $\alpha \in (0,1)$ such that:*

$$\begin{bmatrix} (1-\alpha)\boldsymbol{P} & \boldsymbol{0} & \boldsymbol{F}^T \boldsymbol{P} \\ \boldsymbol{0} & \alpha \boldsymbol{Q}_d & \boldsymbol{G}^T \boldsymbol{P} \\ \boldsymbol{P}\boldsymbol{F} & \boldsymbol{P}\boldsymbol{G} & \boldsymbol{P} \end{bmatrix} \succ 0 \tag{4}$$

The following lemma simplifies the control synthesis task thanks to the elimination of the coupling between the system matrices and the Lyapunov matrix.

**Lemma 2.** *The following statements are equivalent:*

1. *The system (1) is strictly quadratically bounded with $V_k$ for all $\boldsymbol{d}_k \in \mathbb{E}_d$.*
2. *There exist $\alpha \in (0,1)$ and a matrix $\boldsymbol{U}$ such that:*

$$\begin{bmatrix} (\alpha - 1)\boldsymbol{P} & \boldsymbol{0} & \boldsymbol{F}^T \boldsymbol{U}^T \\ \boldsymbol{0} & -\alpha \boldsymbol{Q}_d & \boldsymbol{G}^T \boldsymbol{U}^T \\ \boldsymbol{U}\boldsymbol{F} & \boldsymbol{U}\boldsymbol{G} & \boldsymbol{P} - \boldsymbol{U} - \boldsymbol{U}^T \end{bmatrix} \prec 0 \tag{5}$$

**Proof.** Following the reasoning in de Oliveira, Bernussou, and Geromel (1999), the lemma is proven by noticing that (4) implies (5) when choosing $\boldsymbol{U} = \boldsymbol{U}^T = \boldsymbol{P} \succ 0$. On the other hand, (5) implies (4) by multiplying the former by:

$$\begin{bmatrix} \boldsymbol{I} & \boldsymbol{0} & \boldsymbol{F}^T \\ \boldsymbol{0} & \boldsymbol{I} & \boldsymbol{G}^T \end{bmatrix}$$

on the left and by its transpose on the right. □

The following lemma achieves the elimination of the coupling between the system matrices and the Lyapunov matrix by using the Young's relation (completion of squares), and as such, it introduces some conservativeness in the design, which is unfortunately necessary for obtaining some of the results in the paper.

**Lemma 3.** *Let $\boldsymbol{G}$ and $\boldsymbol{Q}_d$ be partitioned as follows:*

$$\boldsymbol{G} = \begin{bmatrix} \boldsymbol{G}_1 & \boldsymbol{G}_2 \end{bmatrix}, \quad \boldsymbol{Q}_d = \operatorname{diag}\left(\boldsymbol{Q}_d^{(1)}, \boldsymbol{Q}_d^{(2)}\right) \tag{6}$$

*with $\boldsymbol{G}_1 \in \mathbb{R}^{n_z \times 2n_z}$, $\boldsymbol{Q}_d^{(1)} \in \mathbb{S}^{2n_z}$. If there exist $\alpha \in (0,1)$, $\varepsilon > 0$ **and** $\mathcal{P} \in \mathbb{S}^{2n_z}$ such that:*

$$\begin{bmatrix} (1-\alpha)\boldsymbol{P}^{-1} & \boldsymbol{P}^{-1}\boldsymbol{F}^T & \boldsymbol{0} & \boldsymbol{0} & \boldsymbol{0} \\ \boldsymbol{F}\boldsymbol{P}^{-1} & \boldsymbol{P}^{-1} & \boldsymbol{G}_1\mathcal{P}^{-1} & \boldsymbol{G}_2 & \boldsymbol{0} \\ \boldsymbol{0} & \mathcal{P}^{-1}\boldsymbol{G}_1^T & 2\varepsilon\mathcal{P}^{-1} & \boldsymbol{0} & \varepsilon\boldsymbol{I} \\ \boldsymbol{0} & \boldsymbol{G}_2^T & \boldsymbol{0} & \alpha\boldsymbol{Q}_d^{(2)} & \boldsymbol{0} \\ \boldsymbol{0} & \boldsymbol{0} & \varepsilon\boldsymbol{I} & \boldsymbol{0} & \alpha\boldsymbol{Q}_d^{(1)} \end{bmatrix} \succ 0 \tag{7}$$

*then the system (1) is strictly quadratically bounded with $V_k$ for all $\boldsymbol{d}_k \in \mathbb{E}_d$.*

**Proof.** Given (6), the inequality (4) reads as:

$$\begin{bmatrix} (1-\alpha)\boldsymbol{P} & \boldsymbol{0} & \boldsymbol{0} & \boldsymbol{F}^T\boldsymbol{P} \\ \boldsymbol{0} & \alpha\boldsymbol{Q}_d^{(1)} & \boldsymbol{0} & \boldsymbol{G}_1^T\boldsymbol{P} \\ \boldsymbol{0} & \boldsymbol{0} & \alpha\boldsymbol{Q}_d^{(2)} & \boldsymbol{G}_2^T\boldsymbol{P} \\ \boldsymbol{P}\boldsymbol{F} & \boldsymbol{P}\boldsymbol{G}_1 & \boldsymbol{P}\boldsymbol{G}_2 & \boldsymbol{P} \end{bmatrix} \succ 0 \tag{8}$$

which, multiplied by:

$$\begin{bmatrix} \boldsymbol{P}^{-1} & \boldsymbol{0} & \boldsymbol{0} & \boldsymbol{0} \\ \boldsymbol{0} & \boldsymbol{0} & \boldsymbol{0} & \boldsymbol{P}^{-1} \\ \boldsymbol{0} & \mathcal{P}^{-1} & \boldsymbol{0} & \boldsymbol{0} \\ \boldsymbol{0} & \boldsymbol{0} & \boldsymbol{I} & \boldsymbol{0} \end{bmatrix}$$

on the left and its transpose on the right leads to:

$$\begin{bmatrix} (1-\alpha)\boldsymbol{P}^{-1} & \boldsymbol{P}^{-1}\boldsymbol{F}^T & \boldsymbol{0} & \boldsymbol{0} \\ \boldsymbol{F}\boldsymbol{P}^{-1} & \boldsymbol{P}^{-1} & \boldsymbol{G}_1\mathcal{P}^{-1} & \boldsymbol{G}_2 \\ \boldsymbol{0} & \mathcal{P}^{-1}\boldsymbol{G}_1^T & \alpha\mathcal{P}^{-1}\boldsymbol{Q}_d^{(1)}\mathcal{P}^{-1} & \boldsymbol{0} \\ \boldsymbol{0} & \boldsymbol{G}_2^T & \boldsymbol{0} & \alpha\boldsymbol{Q}_d^{(2)} \end{bmatrix} \succ 0 \tag{9}$$

Due to Young's relation, for any matrix $\boldsymbol{Y}$ of appropriate dimensions:

$$\begin{bmatrix} \boldsymbol{0} \\ \boldsymbol{0} \\ \mathcal{P}^{-1} \\ \boldsymbol{0} \end{bmatrix} \alpha\boldsymbol{Q}_d^{(1)} \begin{bmatrix} \boldsymbol{0} \\ \boldsymbol{0} \\ \mathcal{P}^{-1} \\ \boldsymbol{0} \end{bmatrix}^T + \boldsymbol{Y}^T \frac{\left(\boldsymbol{Q}_d^{(1)}\right)^{-1}}{\alpha} \boldsymbol{Y} \succeq \begin{bmatrix} \boldsymbol{0} \\ \boldsymbol{0} \\ \mathcal{P}^{-1} \\ \boldsymbol{0} \end{bmatrix} \boldsymbol{Y} + \boldsymbol{Y}^T \begin{bmatrix} \boldsymbol{0} \\ \boldsymbol{0} \\ \mathcal{P}^{-1} \\ \boldsymbol{0} \end{bmatrix}^T \tag{10}$$

By choosing $\boldsymbol{Y} = \begin{bmatrix} \boldsymbol{0} & \boldsymbol{0} & \varepsilon\boldsymbol{I} & \boldsymbol{0} \end{bmatrix}$, we get that:

$$\begin{bmatrix} (1-\alpha)\boldsymbol{P}^{-1} & \boldsymbol{P}^{-1}\boldsymbol{F}^T & \boldsymbol{0} & \boldsymbol{0} \\ \boldsymbol{F}\boldsymbol{P}^{-1} & \boldsymbol{P}^{-1} & \boldsymbol{G}_1\mathcal{P}^{-1} & \boldsymbol{G}_2 \\ \boldsymbol{0} & \mathcal{P}^{-1}\boldsymbol{G}_1^T & 2\varepsilon\mathcal{P}^{-1} - \frac{\varepsilon^2}{\alpha}\left(\boldsymbol{Q}_d^{(1)}\right)^{-1} & \boldsymbol{0} \\ \boldsymbol{0} & \boldsymbol{G}_2^T & \boldsymbol{0} & \alpha\boldsymbol{Q}_d^{(2)} \end{bmatrix} \succ 0 \tag{11}$$

implies (9) (although the converse is not true). Note that, by inspecting (11), necessarily:

$$2\varepsilon\mathcal{P}^{-1} - \frac{\varepsilon^2}{\alpha}\left(\boldsymbol{Q}_d^{(1)}\right)^{-1} \succ 0 \tag{12}$$

which can be true only if $\varepsilon > 0$. By applying Schur complement to (11), we obtain (7), thus completing the proof. □

**Lemma 4.** *If the system (1) is strictly quadratically bounded with $V_k$ for all $\boldsymbol{d}_k \in \mathbb{E}_d$, then there exists $\alpha \in (0,1)$ such that:*

$$V_k < (1-\alpha)^k V_0 \quad \textit{for } \boldsymbol{d}_k = \boldsymbol{0} \tag{13}$$

**Proof.** For $\boldsymbol{d}_k = \boldsymbol{0}$, the inequality (2) reduces to $V_{k+1} < (1-\alpha)V_k$ when $\boldsymbol{d}_k = \boldsymbol{0}$ which, by induction, leads to (13). □

## 3. Problem formulation

The objective of this section is to describe the ingredients of the FTC scheme presented in Fig. 1:

- the system modelled as constrained linear-time invariant model affected by disturbances and possibly faults,
- the deterministic reference model,
- the fault and state estimator, and
- the fault-tolerant controller.

The considered system is described by the following discrete-time model considering faults and disturbances:

$$\boldsymbol{x}_{k+1} = \boldsymbol{A}\boldsymbol{x}_k + \boldsymbol{B}\boldsymbol{u}_k + \boldsymbol{B}\boldsymbol{f}_{a,k} + \boldsymbol{W}\boldsymbol{w}_k \tag{14}$$

$$\boldsymbol{y}_k = \boldsymbol{C}\boldsymbol{x}_k + \boldsymbol{V}\boldsymbol{v}_k \tag{15}$$

where $\boldsymbol{x}_k \in \mathbb{X} \subset \mathbb{R}^{n_x}$, $\boldsymbol{u}_k \in \mathbb{U} \subset \mathbb{R}^{n_u}$ are the constrained state and input with:

$$\mathbb{X} = \{\boldsymbol{x} : \underline{x}_i \le x_{i,k} \le \bar{x}_i, \quad i = 1, \dots, n_x\} \tag{16}$$

$$\mathbb{U} = \{\boldsymbol{u} : \underline{u}_j \le u_{j,k} \le \bar{u}_j, \quad j = 1, \dots, n_u\} \tag{17}$$

while $\underline{x}_i < \bar{x}_i$ and $\underline{u}_j < \bar{u}_j$. Moreover, $\boldsymbol{f}_{a,k} \in \mathbb{F}_a \subset \mathbb{R}^{n_f}$ denotes the actuator fault and its possible time-evolution bounded within an ellipsoid $\boldsymbol{\epsilon}_k = \boldsymbol{f}_{a,k+1} - \boldsymbol{f}_{a,k} \in \mathbb{E}_\epsilon \subset \mathbb{R}^{n_f}$. Subsequently, $\boldsymbol{w}_k \in \mathbb{E}_w \subset \mathbb{R}^{n_w}$ and $\boldsymbol{v}_k \in \mathbb{E}_v \subset \mathbb{R}^{n_v}$ stand for the ellipsoidally bounded exogenous external disturbances, which can model several uncertainties, e.g. unmodelled system dynamics. Furthermore, the matrices $\boldsymbol{B}$, $\boldsymbol{C}$ are assumed to be full rank and $n_u \le n_y$. The last fact implies that it is impossible to estimate more faults than the measured outputs. The input of the possibly faulty system (14)–(15) should be designed in such a way that $\boldsymbol{x}_k$ tracks the reference state $\boldsymbol{x}_{r,k}$, which obeys the following reference model:

$$\boldsymbol{x}_{r,k+1} = \boldsymbol{A}\boldsymbol{x}_{r,k} + \boldsymbol{B}\boldsymbol{u}_{r,k} + \boldsymbol{B}\hat{\boldsymbol{f}}_{a,k} \tag{18}$$

$$\boldsymbol{y}_{r,k} = \boldsymbol{C}\boldsymbol{x}_{r,k} \tag{19}$$

$$\boldsymbol{z}_{r,k} = \boldsymbol{H}\boldsymbol{x}_{r,k} \tag{20}$$

where $\boldsymbol{z}_{r,k} \in \mathbb{R}^{n_z}$ while $n_z \le n_u$. The dimensions of the remaining variables are the same as in (14)–(15). Moreover, the system (18)–(20) should follow the reference $\boldsymbol{r}_k$, i.e., $\boldsymbol{z}_k$ should converge to $\boldsymbol{r}_k$. The reference $\boldsymbol{r}_k$ is assumed to be available on a finite preview horizon $n_h$, i.e. $\boldsymbol{r}_k, \dots, \boldsymbol{r}_{k+n_h-1}$ are known. Contrarily to the approaches presented in the literature (Lan & Patton, 2021; Witczak et al., 2013), the reference model (18)–(20) explicitly incorporates the fault estimate $\hat{\boldsymbol{f}}_{a,k}$. While this might appear to impair the reference model's independence and potentially its ability to directly attain the desired output trajectory $\boldsymbol{r}_k$, this inclusion is a deliberate and beneficial design choice. It allows the feedforward control action $\boldsymbol{u}_{r,k}$ to be dynamically reconfigured based on the estimated fault magnitude, thus distributing the compensation effort between feedforward and feedback control components. In doing so, part of the fault's effect is proactively mitigated at the reference trajectory generation stage, which improves tracking and reduces the correction burden on the feedback controller. The key advantage of this structure, beyond enabling more responsive compensation, is that it allows feasibility of control actions to be assessed directly at the reference model level (18)–(20), rather than through the faulty system dynamics (14)–(15). As a result, the reference trajectory $\boldsymbol{r}_k$ can be modified in a principled way to ensure constraint satisfaction and reliable

tracking, offering a significant improvement over existing methods (Lan & Patton, 2022).

Subsequently, let us define a state and fault estimator that estimate $\hat{\boldsymbol{x}}_k$ and $\hat{\boldsymbol{f}}_{a,k}$ as follows:

$$\hat{\boldsymbol{x}}_{k+1} = \boldsymbol{A}\hat{\boldsymbol{x}}_k + \boldsymbol{B}\boldsymbol{u}_k + \boldsymbol{B}\hat{\boldsymbol{f}}_{a,k} + \boldsymbol{L}\left(\boldsymbol{y}_k - \boldsymbol{C}\hat{\boldsymbol{x}}_k\right) \tag{21}$$

$$\hat{\boldsymbol{f}}_{a,k+1} = \hat{\boldsymbol{f}}_{a,k} + \boldsymbol{F}\left(\boldsymbol{y}_k - \boldsymbol{C}\hat{\boldsymbol{x}}_k\right) \tag{22}$$

where $\boldsymbol{L}$ and $\boldsymbol{F}$ are the estimator gain matrices while the integrated control strategy has the form:

$$\boldsymbol{u}_k = -\boldsymbol{K}(\hat{\boldsymbol{x}}_k - \boldsymbol{x}_{r,k}) + \boldsymbol{u}_{r,k} \tag{23}$$

Note that although the control input $\mathbf{u}_k$ in (23) does not explicitly depend on the fault estimate $\hat{\mathbf{f}}_{a,k}$, the overall control action is indeed influenced by it through multiple indirect pathways. The observer state $\hat{\mathbf{x}}_k$ is updated via (21), which includes $\hat{\mathbf{f}}_{a,k}$, and the reference trajectory $\boldsymbol{x}_{r,k}$ and feedforward term $\boldsymbol{u}_{r,k}$ are computed using a reference model that incorporates the fault estimate, as discussed earlier. This architecture allows the controller to react to faults through feedforward reconfiguration and estimation-driven state correction, without requiring explicit fault terms in the feedback gain. This design is particularly suited for additive actuator faults which, unlike multiplicative or parametric faults, do not compromise closed-loop stability making the direct reconfiguration of the controller gain unnecessary.

The main difficulty lies in the fact that the effect of an unknown $\boldsymbol{f}_{a,k}$ should be accommodated taking into account a bounded performance of the actuators expressed by (17). Indeed, contrarily to other approaches presented in the literature (Lan & Patton, 2016a), a conservative assumption regarding the ability of compensating an actuator fault with the same faulty actuator is eliminated. Instead, a suitable control allocation among the available actuators is implemented, which will guarantee a possibly efficient fault accommodation. For the purpose of further deliberations, let us define error variables as $\boldsymbol{e}_k = \boldsymbol{x}_k - \hat{\boldsymbol{x}}_k$ (state estimation error), $\boldsymbol{e}_{a,k} = \boldsymbol{f}_{a,k} - \hat{\boldsymbol{f}}_{a,k}$ (actuator fault estimation error), and $\boldsymbol{e}_{r,k} = \boldsymbol{x}_k - \boldsymbol{x}_{r,k}$ (real tracking error). Thus, by a manipulation of (14)–(15), (18)–(19) and (23), one can obtain the following overall dynamics of the error variables:

$$\boldsymbol{e}_{r,k+1} = (\boldsymbol{A} - \boldsymbol{B}\boldsymbol{K})\boldsymbol{e}_{r,k} + \boldsymbol{B}\boldsymbol{K}\boldsymbol{e}_k + \boldsymbol{B}\boldsymbol{e}_{a,k} + \boldsymbol{W}\boldsymbol{w}_k \tag{24}$$

$$\boldsymbol{e}_{k+1} = (\boldsymbol{A} - \boldsymbol{L}\boldsymbol{C})\boldsymbol{e}_k + \boldsymbol{B}\boldsymbol{e}_{a,k} + \boldsymbol{W}\boldsymbol{w}_k - \boldsymbol{L}\boldsymbol{V}\boldsymbol{v}_k \tag{25}$$

$$\boldsymbol{e}_{a,k+1} = \boldsymbol{e}_{a,k} - \boldsymbol{F}\boldsymbol{C}\boldsymbol{e}_k - \boldsymbol{F}\boldsymbol{V}\boldsymbol{v}_k + \boldsymbol{\varepsilon}_k \tag{26}$$

The objective of the subsequent section is to propose an integrated and simultaneous design of (21)–(23) based on (24)–(26) considering the scheme presented in Fig. 1.

## 4. Integrated FTC design

As detailed in Lan and Patton (2021), the simultaneous design of the estimator and controller is not an easy task. Indeed, Lan and Patton (2021) proposes an approximated remedy to this problem. This section proposes a less conservative approach. First, let us reshape (24) and (25)–(26) into equivalent forms that fit the equation structure (1):

$$\boldsymbol{e}_{r,k+1} = (\boldsymbol{A} - \boldsymbol{B}\boldsymbol{K})\boldsymbol{e}_{r,k} + \begin{bmatrix}\boldsymbol{B}\boldsymbol{K} & \boldsymbol{B} & \boldsymbol{W}\end{bmatrix}\tilde{\boldsymbol{w}}_k \tag{27}$$

$$\bar{\boldsymbol{e}}_{k+1} = (\bar{\boldsymbol{A}} - \bar{\boldsymbol{L}}\bar{\boldsymbol{C}})\bar{\boldsymbol{e}}_k + \begin{bmatrix}-\bar{\boldsymbol{L}}\boldsymbol{V} & \bar{\boldsymbol{W}} & \bar{\boldsymbol{I}}\end{bmatrix}\tilde{\boldsymbol{v}}_k \tag{28}$$

where $\bar{\boldsymbol{e}}_k = [\boldsymbol{e}_k^T, \boldsymbol{e}_{a,k}^T]^T$, $\tilde{\boldsymbol{w}}_k = [\bar{\boldsymbol{e}}_k^T, \boldsymbol{w}_k^T]^T$, $\tilde{\boldsymbol{v}}_k = [\boldsymbol{v}_k^T, \boldsymbol{w}_k^T, \boldsymbol{\epsilon}_k^T]^T$, and:

$$\bar{\boldsymbol{A}} = \begin{bmatrix}\boldsymbol{A} & \boldsymbol{B}\\ \boldsymbol{0} & \boldsymbol{I}\end{bmatrix}, \bar{\boldsymbol{L}} = \begin{bmatrix}\boldsymbol{L}\\ \boldsymbol{F}\end{bmatrix}, \bar{\boldsymbol{C}} = \begin{bmatrix}\boldsymbol{C} & \boldsymbol{0}\end{bmatrix}, \bar{\boldsymbol{W}} = \begin{bmatrix}\boldsymbol{W}\\ \boldsymbol{0}\end{bmatrix}, \bar{\boldsymbol{I}} = \begin{bmatrix}\boldsymbol{0}\\ \boldsymbol{I}\end{bmatrix}$$

Note that the signal $\tilde{\boldsymbol{v}}_k$ is bounded within an ellipsoid $\mathbb{E}_{\tilde{\boldsymbol{v}}}$, defined by the matrix $\boldsymbol{Q}_{\tilde{v}} = \frac{1}{3}\mathrm{diag}(\boldsymbol{Q}_v, \boldsymbol{Q}_w, \boldsymbol{Q}_\varepsilon)$. Also, as long as one guarantees that the signal $\bar{\boldsymbol{e}}_k$ is bounded within an ellipsoid $\mathbb{E}_{\bar{\boldsymbol{e}},\boldsymbol{P}_e}$, then also $\tilde{\boldsymbol{w}}_k$ is bounded within $\mathbb{E}_{\tilde{\boldsymbol{w}}}$, $\boldsymbol{Q}_{\tilde{w}} = \frac{1}{2}\mathrm{diag}(\boldsymbol{P}_e, \boldsymbol{Q}_w)$.

The most common design approach used in the literature (Lan & Patton, 2016b, 2022) is to merge $\boldsymbol{e}_{r,k}$ and $\bar{\boldsymbol{e}}_k$ into one vector and then prove the convergence of the overall augmented system. This paper provides an alternative solution, by means of the following theorem, which constitutes the main result of this section. It should be also noted that for the nondeterministic system (14)–(15) the so-called separation principle does not hold and hence the controller and fault estimator cannot be designed separately.

**Theorem 1.** *Let there exist $\alpha_e \in (0,1)$, $\alpha_c \in (0,1)$, $\varepsilon_c > 0$, $\boldsymbol{P}_e \succ 0$, $\boldsymbol{R}_c \succ 0$, $\boldsymbol{R}_a \succ 0$, $\boldsymbol{U}_e$, $\boldsymbol{N}_e$, $\boldsymbol{N}_c$ such that:*

$$\begin{bmatrix}(\alpha_e-1)\boldsymbol{P}_e & \boldsymbol{0} & \boldsymbol{0} & \boldsymbol{0} & \bar{\boldsymbol{A}}^T\boldsymbol{U}_e^T - \bar{\boldsymbol{C}}^T\boldsymbol{N}_e^T\\ \boldsymbol{0} & -\frac{1}{3}\alpha_e\boldsymbol{Q}_v & \boldsymbol{0} & \boldsymbol{0} & -\boldsymbol{V}^T\boldsymbol{N}_e^T\\ \boldsymbol{0} & \boldsymbol{0} & -\frac{1}{3}\alpha_e\boldsymbol{Q}_w & \boldsymbol{0} & \bar{\boldsymbol{W}}^T\boldsymbol{U}_e^T\\ \boldsymbol{0} & \boldsymbol{0} & \boldsymbol{0} & -\frac{1}{3}\alpha_e\boldsymbol{Q}_\varepsilon & \bar{\boldsymbol{I}}^T\boldsymbol{U}_e^T\\ \boldsymbol{U}_e\bar{\boldsymbol{A}} - \boldsymbol{N}_e\bar{\boldsymbol{C}} & -\boldsymbol{N}_e\boldsymbol{V} & \boldsymbol{U}_e\bar{\boldsymbol{W}} & \boldsymbol{U}_e\bar{\boldsymbol{I}} & \boldsymbol{P}_e - \boldsymbol{U}_e - \boldsymbol{U}_e^T\end{bmatrix} \prec 0 \tag{29}$$

$$\begin{bmatrix}(1-\alpha_c)\boldsymbol{R}_c & \boldsymbol{R}_c\boldsymbol{A}^T - \boldsymbol{N}_c^T\boldsymbol{B}^T & \boldsymbol{0} & \boldsymbol{0} & \boldsymbol{0}\\ \boldsymbol{A}\boldsymbol{R}_c - \boldsymbol{B}\boldsymbol{N}_c & \boldsymbol{R}_c & \begin{bmatrix}\boldsymbol{B}\boldsymbol{N}_c & \boldsymbol{B}\boldsymbol{R}_a\end{bmatrix} & \boldsymbol{W} & \boldsymbol{0}\\ \boldsymbol{0} & \begin{bmatrix}\boldsymbol{B}\boldsymbol{N}_c & \boldsymbol{B}\boldsymbol{R}_a\end{bmatrix}^T & 2\varepsilon_c\mathrm{diag}(\boldsymbol{R}_c, \boldsymbol{R}_a) & \boldsymbol{0} & \varepsilon_c\boldsymbol{I}\\ \boldsymbol{0} & \boldsymbol{W}^T & \boldsymbol{0} & \frac{\alpha_c}{2}\boldsymbol{Q}_w & \boldsymbol{0}\\ \boldsymbol{0} & \boldsymbol{0} & \varepsilon_c\boldsymbol{I} & \boldsymbol{0} & \frac{\alpha_c}{2}\boldsymbol{P}_e\end{bmatrix} \succ 0 \tag{30}$$

*Then, the systems (27)–(28) with $\bar{\boldsymbol{L}} = \boldsymbol{U}_e^{-1}\boldsymbol{N}_e$ and $\boldsymbol{K} = \boldsymbol{N}_c\boldsymbol{R}_c^{-1}$ are strictly quadratically bounded with $V_k = \bar{\boldsymbol{e}}_k^T\boldsymbol{P}_e\bar{\boldsymbol{e}}_k$ and $V_k = \boldsymbol{e}_{r,k}^T\boldsymbol{P}_c\boldsymbol{e}_{r,k}$, respectively, with $\boldsymbol{P}_c = \boldsymbol{R}_c^{-1}$, for all $\boldsymbol{w}_k \in \mathbb{E}_w$, $\boldsymbol{v}_k \in \mathbb{E}_v$ and $\boldsymbol{\varepsilon}_k \in \mathbb{E}_\varepsilon$.*

**Proof.** By applying Lemma 2 to (28), with $\boldsymbol{F} = \bar{\boldsymbol{A}} - \bar{\boldsymbol{L}}\bar{\boldsymbol{C}}$ and $\boldsymbol{G} = \begin{bmatrix}-\bar{\boldsymbol{L}}\boldsymbol{V} & \bar{\boldsymbol{W}} & \bar{\boldsymbol{I}}\end{bmatrix}$, one finds that its strict quadratic boundedness with $V_k = \bar{\boldsymbol{e}}_k^T\boldsymbol{P}_e\bar{\boldsymbol{e}}_k$ for all $\tilde{\boldsymbol{v}}_k \in \mathbb{E}_{\tilde{\boldsymbol{v}},\boldsymbol{Q}_{\tilde{v}}}$ is equivalent to the existence of some $\alpha_e \in (0,1)$ and a matrix $\boldsymbol{U}_e$ such that (31) holds.

$$\begin{bmatrix}(\alpha_e-1)\boldsymbol{P}_e & \boldsymbol{0} & \left(\bar{\boldsymbol{A}}^T - \bar{\boldsymbol{C}}^T\bar{\boldsymbol{L}}^T\right)\boldsymbol{U}_e^T\\ \boldsymbol{0} & -\alpha_e\boldsymbol{Q}_{\tilde{v}} & \begin{bmatrix}-\bar{\boldsymbol{L}}\boldsymbol{V} & \bar{\boldsymbol{W}} & \bar{\boldsymbol{I}}\end{bmatrix}^T\boldsymbol{U}_e^T\\ \boldsymbol{U}_e\left(\bar{\boldsymbol{A}} - \bar{\boldsymbol{L}}\bar{\boldsymbol{C}}\right) & \boldsymbol{U}_e\begin{bmatrix}-\bar{\boldsymbol{L}}\boldsymbol{V} & \boldsymbol{W} & \boldsymbol{I}\end{bmatrix} & \boldsymbol{P}_e - \boldsymbol{U}_e - \boldsymbol{U}_e^T\end{bmatrix} \prec 0 \tag{31}$$

By accounting for $\boldsymbol{Q}_{\tilde{v}} = \frac{1}{3}\mathrm{diag}(\boldsymbol{Q}_v, \boldsymbol{Q}_w, \boldsymbol{Q}_\varepsilon)$ and by applying the linearizing change of variables $\boldsymbol{N}_e = \boldsymbol{U}_e\bar{\boldsymbol{L}}$, (29) is obtained.

On the other hand, by applying Lemma 3 with $\boldsymbol{F} = \boldsymbol{A} - \boldsymbol{B}\boldsymbol{K}$, $\boldsymbol{G}_1 = \begin{bmatrix}\boldsymbol{B}\boldsymbol{K} & \boldsymbol{B}\end{bmatrix}$, $\boldsymbol{G}_2 = \boldsymbol{W}$, $\boldsymbol{Q}_d^{(1)} = \frac{1}{2}\boldsymbol{P}_e$, $\boldsymbol{Q}_d^{(2)} = \frac{1}{2}\boldsymbol{Q}_w$, strict quadratic boundedness of (27) with $V_k = \boldsymbol{e}_{r,k}^T\boldsymbol{P}_c\boldsymbol{e}_{r,k}$ for all $\tilde{\boldsymbol{w}}_k \in \mathbb{E}_{\tilde{\boldsymbol{w}}}$ is ensured by the existence of $\alpha_c \in (0,1)$, $\varepsilon_c > 0$, **and** $\mathcal{P}_c \in \mathbb{R}^{2n_x}$ such that:

$$\begin{bmatrix}(1-\alpha_c)\boldsymbol{P}_c^{-1} & \boldsymbol{P}_c^{-1}(\boldsymbol{A} - \boldsymbol{B}\boldsymbol{K})^T & \boldsymbol{0} & \boldsymbol{0} & \boldsymbol{0}\\ (\boldsymbol{A} - \boldsymbol{B}\boldsymbol{K})\boldsymbol{P}_c^{-1} & \boldsymbol{P}_c^{-1} & \begin{bmatrix}\boldsymbol{B}\boldsymbol{K} & \boldsymbol{B}\end{bmatrix}\mathcal{P}_c^{-1} & \boldsymbol{W} & \boldsymbol{0}\\ \boldsymbol{0} & \mathcal{P}_c^{-1}\begin{bmatrix}\boldsymbol{B}\boldsymbol{K} & \boldsymbol{B}\end{bmatrix}^T & 2\varepsilon_c\mathcal{P}_c^{-1} & \boldsymbol{0} & \varepsilon_c\boldsymbol{I}\\ \boldsymbol{0} & \boldsymbol{W}^T & \boldsymbol{0} & \frac{\alpha_c}{2}\boldsymbol{Q}_w & \boldsymbol{0}\\ \boldsymbol{0} & \boldsymbol{0} & \varepsilon_c\boldsymbol{I} & \boldsymbol{0} & \frac{\alpha_c}{2}\boldsymbol{P}_e\end{bmatrix} \succ 0 \tag{32}$$

By choosing $\mathcal{P}_c = \mathrm{diag}\left(\boldsymbol{P}_c, \boldsymbol{P}_a\right)$, defining $\boldsymbol{R}_c = \boldsymbol{P}_c^{-1}$, $\boldsymbol{R}_a = \boldsymbol{P}_a^{-1}$, and applying the linearizing change of variables $\boldsymbol{N}_c = \boldsymbol{K}\boldsymbol{R}_c$, (30) is obtained, thus completing the proof. □

**Theorem 2.** *If the systems (27) and (28) are strictly quadratically bounded with $V_k = \boldsymbol{e}_{r,k}^T\boldsymbol{P}_c\boldsymbol{e}_{r,k}$ and $V_k = \bar{\boldsymbol{e}}_k^T\boldsymbol{P}_e\bar{\boldsymbol{e}}_k$ for all $\tilde{\boldsymbol{w}}_k \in \mathbb{E}_{\tilde{\boldsymbol{w}}}$ and $\tilde{\boldsymbol{v}}_k \in \mathbb{E}_{\tilde{\boldsymbol{v}}}$, respectively, then there exist $\alpha_c \in (0,1)$ and $\alpha_e \in (0,1)$ such that:*

$$\boldsymbol{e}_{r,k}^T\boldsymbol{P}_c\boldsymbol{e}_{r,k} < (1-\alpha_c)^k\boldsymbol{e}_{r,0}^T\boldsymbol{P}_c\boldsymbol{e}_{r,0} \quad \text{for } \tilde{\boldsymbol{w}}_k = \boldsymbol{0}, \tag{33}$$

$$\bar{\boldsymbol{e}}_k^T\boldsymbol{P}_e\bar{\boldsymbol{e}}_k < (1-\alpha_e)^k\bar{\boldsymbol{e}}_0^T\boldsymbol{P}_e\bar{\boldsymbol{e}}_0 \quad \text{for } \tilde{\boldsymbol{v}}_k = \boldsymbol{0}, \tag{34}$$

**Proof.** The proof is a straightforward application of Lemma 4. □

The above theorem clearly shows that the exponential convergence can be achieved for $\tilde{\boldsymbol{w}}_k = \boldsymbol{0}$ and $\tilde{\boldsymbol{v}}_k = \boldsymbol{0}$. Additionally, it provides a concise interpretation of the design parameters $\alpha_c$ and $\alpha_e$.

## 5. Towards two-stage design procedure

The objective of this section is to provide the final integration procedure of the scheme in Fig. 1 including MPC for the reference system.

### 5.1. Stage I: Off-line determination of integrated FTC

Let us start with noting the fact that for fixed $\alpha_e \in (0,1)$, $\alpha_c \in (0,1)$, $\varepsilon_c > 0$, the matrix inequalities (29)–(30) become two distinct LMIs which are computationally efficient to solve. The conventional methods in the literature (see, for example, Lan and Patton (2021) and the references therein) call for a single diagonal Lyapunov matrix, which is linked to a rather large LMI that incorporates controller and estimator design parameters. Therefore, compared to state-of-the-art techniques, it is clear that the suggested strategy reduces both conservativeness and complexity (Lan & Patton, 2021). It follows directly from Theorem 2 that the larger $\alpha_e$ and $\alpha_c$ are, the faster the convergence of the error variables $\bar{\boldsymbol{e}}_k$ and $\boldsymbol{e}_{r,k+1}$. On the other hand, the matrices $\boldsymbol{P}_e$ and $\boldsymbol{R}_c$ determine the ellipsoidal invariant set for $\bar{\boldsymbol{e}}_k$ and $\boldsymbol{e}_{r,k+1}$, respectively. These sets can be perceived as uncertainty regions, which should be as small as possible. Thus, one can, minimize some geometrical measures, e.g., the volume which is equivalent to maximizing the determinants of matrices $\boldsymbol{P}_e$ and $\boldsymbol{P}_c$, the latter corresponding to minimization of the determinant of the matrix $\boldsymbol{R}_c$. By denoting the selected criteria by $J(\alpha_c, \alpha_e, \boldsymbol{P}_e, \boldsymbol{R}_c)$, an offline iterative procedure can be easily implemented, which alternates the following steps:

1. Select $\alpha_e \in (0,1)$, $\alpha_c \in (0,1)$, $\varepsilon_c \in (0, \bar{\varepsilon}_c)$.
2. Optimize $J(\alpha_c, \alpha_e, \varepsilon_c, \boldsymbol{P}_e, \boldsymbol{R}_c)$ under (29)–(30).

where $\bar{\varepsilon}_c > 0$ is a design parameter. It should be noted that $J(\alpha_c, \alpha_e, \varepsilon, \boldsymbol{P}_e, \boldsymbol{R}_c)$ might include both the control and estimation uncertainty ellipsoidal areas and the convergence rates $(\alpha_c, \alpha_e)$. Since $\boldsymbol{P}_e$ and $\boldsymbol{R}_c$ form these regions, one can minimize either the estimation or control uncertainty sets, for example, by optimizing their determinants. This tactic offers a means of strengthening the resilience of the suggested approach.

The above strategy can be directly implemented using brute force search within 3-dimensional bounded set $\alpha_e \in (0,1)$, $\alpha_c \in (0,1)$, $\varepsilon_c \in (0, \bar{\varepsilon}_c)$ using a grid of desired sparsity. Of course, more specialized searching methods can be used instead, e.g. branch and bound strategy (Morrison, Jacobson, Sauppe, & Sewell, 2016).

### 5.2. Stage II: On-line determination of reference and FTC

Let us define the observed tracking error as $\boldsymbol{e}_{t,k} = \hat{\boldsymbol{x}}_k - \boldsymbol{x}_{r,k}$, which is linked to previously defined error variables according to $\boldsymbol{e}_{t,k} = \boldsymbol{e}_{r,k} - \boldsymbol{e}_k$. From (17) and (23), it is evident that:

$$\mathbb{U}_{r,k} = \{\boldsymbol{u}_{r,k} : \underline{u}_j + \boldsymbol{K}_j \boldsymbol{e}_{t,k} \le u_{r,j,k} \le \bar{u}_j + \boldsymbol{K}_j \boldsymbol{e}_{t,k}, \quad j = 1, \dots, n_u\} \tag{35}$$

where $\boldsymbol{K}_j$ is the $j$th row of $\boldsymbol{K}$. Thus, the objective is to determine $\boldsymbol{u}_{r,k}$ satisfying (35), which would lead to $\boldsymbol{u}_k$ obeying (17). Note that contrarily to the real tracking error $\boldsymbol{e}_{r,k}$ which cannot be directly computed, the observed tracking error $\boldsymbol{e}_{t,k}$ can be reconstructed from available data. On the other hand, its future one-step update $\boldsymbol{e}_{t,k+1}$ can be obtained by combining together (24)–(25):

$$\boldsymbol{e}_{t,k+1} = (\boldsymbol{A} - \boldsymbol{B}\boldsymbol{K})\boldsymbol{e}_{t,k} + \boldsymbol{L}(\boldsymbol{y}_k - \boldsymbol{C}\hat{\boldsymbol{x}}_k) \tag{36}$$

However, without knowing $\boldsymbol{y}_{k+\ell}$ and $\hat{\boldsymbol{x}}_{k+\ell}$, $\ell > 1$ the determination of $\boldsymbol{e}_{t,k+\ell}$ for $\ell > 1$ is impossible, and hence, its worst case values should be used instead. Since the quadratic boundedness constraints, $\boldsymbol{e}_{r,k}$ and $\bar{\boldsymbol{e}}_k$ satisfy $\boldsymbol{e}_{r,k}^T \boldsymbol{P}_c \boldsymbol{e}_{r,k} \le 1$ and $\bar{\boldsymbol{e}}_k^T \boldsymbol{P}_e \bar{\boldsymbol{e}}_k \le 1$. Thus, it follows that $\boldsymbol{e}_{r,k} \in [-\boldsymbol{r}, \boldsymbol{r}]$ and $\bar{\boldsymbol{e}}_k \in [-\boldsymbol{b}, \boldsymbol{b}]$ with $\boldsymbol{r} = \operatorname{diag}\left(\boldsymbol{P}_c^{-1/2}\right)$ and $\boldsymbol{b} = \operatorname{diag}\left(\boldsymbol{P}_e^{-1/2}\right)$, where the inclusion is meant elementwise. Note that by partitioning $\boldsymbol{b}$ as $\boldsymbol{b}^T = \left[\boldsymbol{b}_1^T, \boldsymbol{b}_2^T\right]^T$, where $\boldsymbol{b}_1$ has the same dimension as $\boldsymbol{r}$, then $\boldsymbol{e}_k \in [-\boldsymbol{b}_1, \boldsymbol{b}_1]$. Consequently, at each sample $k$ one can determine an outer-bounding set $\bar{\mathbb{U}}_{r,k+\ell}$ for $\mathbb{U}_{r,k+\ell}$ as follows:

$$\bar{\mathbb{U}}_{r,k+\ell} = \{\boldsymbol{u}_{r,k+\ell} : \underline{u}_j + \underline{\delta}_{j,k+\ell} \le u_{r,j,k+\ell} \le \bar{u}_j + \bar{\delta}_{j,k+\ell}, \quad j = 1, \dots, n_u\} \tag{37}$$

where:

$$\underline{\delta}_{j,k+\ell} = \begin{cases} \boldsymbol{K}_j \boldsymbol{e}_{t,k+\ell} & \text{for } \ell \in \{0,1\}, \\ |\boldsymbol{K}_j|\left(\boldsymbol{r} + \boldsymbol{b}_1\right) & \text{otherwise} \end{cases} \tag{38}$$

and:

$$\bar{\delta}_{j,k+\ell} = \begin{cases} \boldsymbol{K}_j \boldsymbol{e}_{t,k+\ell} & \text{for } \ell \in \{0,1\}, \\ -|\boldsymbol{K}_j|\left(\boldsymbol{r} + \boldsymbol{b}_1\right) & \text{otherwise} \end{cases} \tag{39}$$

Subsequently, since $\boldsymbol{x}_{r,k} = \boldsymbol{x}_k - \boldsymbol{e}_{r,k}$, (16) leads to:

$$\mathbb{X}_{r,k+\ell} = \{\boldsymbol{x}_{r,k+\ell} : \underline{x}_i - e_{r,i,k+\ell} \le x_{r,i,k+\ell} \le \bar{x}_i - e_{r,i,k+\ell}, \quad i = 1, \dots, n_x\}$$

while its outer-bounding set, i.e. $\mathbb{X}_{r,k+\ell} \subseteq \bar{\mathbb{X}}_{r,k+\ell}$ is:

$$\bar{\mathbb{X}}_{r,k+\ell} = \{\boldsymbol{x}_{r,k+\ell} : \underline{x}_i + r_i \le x_{r,i,k+\ell} \le \bar{x}_i - r_i, \quad i = 1, \dots, n_x\} \tag{40}$$

The availability of the admissible sets (35) and (40) for the reference input $\boldsymbol{u}_{r,k+\ell}$ and the reference state $\boldsymbol{x}_{r,k+\ell}$, respectively, allows for the obtention of an algorithm that determines a suitable $\boldsymbol{u}_{r,k}$ such that the output (20), i.e. $\boldsymbol{z}_{r,k} = \boldsymbol{H}\boldsymbol{x}_{r,k}$ tracks a given reference signal $\boldsymbol{r}_k$. For that purpose, a general model predictive control (MPC) paradigm is used (Camacho & Bordons, 2007; Magni, Raimondo, & Scattolini, 2006). The main reason behind using MPC is that it is well suited for handling the above-defined time-varying input and state constraints. Additionally, it allows tracking of the reference signal that varies over time while minimizing some predefined cost function. Let us start with introducing the *unknown* reference state sequence:

$$\boldsymbol{x}_{r,[t_1,t_2]} = [\boldsymbol{x}_{r,t_1}, \boldsymbol{x}_{r,t_1+1}, \dots, \boldsymbol{x}_{r,t_2}],$$

the *unknown* reference input sequence:

$$\boldsymbol{u}_{r,[t_1,t_2]} = [\boldsymbol{u}_{r,t_1}, \boldsymbol{u}_{r,t_1+1}, \dots, \boldsymbol{u}_{r,t_2}],$$

and the *known* reference trajectory sequence:

$$\boldsymbol{r}_{[t_1,t_2]} = [\boldsymbol{r}_{t_1}, \boldsymbol{r}_{t_1+1}, \dots, \boldsymbol{r}_{t_2}],$$

with $t_2 \ge t_1$. Following Camacho and Bordons (2007) and Magni et al. (2006), let us define over a prediction horizon $N_p$ the stage cost $\mathcal{L}(\boldsymbol{x}_r, \boldsymbol{r}, \boldsymbol{u}_r)$, the terminal penalty $V_f(\boldsymbol{x}_r)$ and the terminal set $\mathbb{X}_f$. Note that the classical MPC stage cost has a quadratic form. Additionally, let us assume that the actuator fault will be constant over the entire prediction horizon, so that the future actuator fault estimate is equal to the present estimate $\hat{\boldsymbol{f}}_{a,k+\ell} = \hat{\boldsymbol{f}}_{a,k}$, $\ell = 0, \dots, N_p - 1$. As a result, the optimization problem is as follows.

**Optimization problem:** *Given the prediction horizon $N_p$ and the reference trajectory sequence $\boldsymbol{r}_{[k,k+N_p-1]}$, minimize:*

$$J = \sum_{t=k}^{k+N_p-1} \mathcal{L}(\boldsymbol{x}_{r,t}, \boldsymbol{r}_t, \boldsymbol{u}_{r,t}) + V_f(\boldsymbol{x}_{r,k+N_p})$$

*with respect to $\boldsymbol{u}_{r,[k,k+N_p-1]}$, under the following constraints:*

- *the reference system dynamics (18);*
- *the input and state constraints (37) and (40), $\ell = 0, 1, \dots, N_p - 1$;*
- *the terminal state constraint $\boldsymbol{x}_{r,k+N_p} \in \mathbb{X}_f$.*

The above MPC algorithm can be implemented using several strategies (Camacho & Bordons, 2007). One way to settle this issue is to use a suitable Matlab MPC toolbox. Irrespective of the selected approach, the final step-by-step on-line operational procedure reduces to repeating cyclically the following steps:

**Fig. 2.** A two-tank system.

1. Obtain state and actuator fault estimates with (21)–(22);
2. Solve the above optimization problem to determine the input sequence $\boldsymbol{u}_{r,[k,k+N_p-1]}$ and, through the reference system dynamics (18), the corresponding reference state $\boldsymbol{x}_{r,[k+1,k+N_p]}$;
3. Feed the system (14) with the FTC law (23) using $\boldsymbol{u}_r(t) = \boldsymbol{u}_r(t_k),\ t \in [t_k, t_{k+1})$.

The proposed strategy works under the following assumptions

- The system (14)–(15) is controllable and observable.
- The above-defined MPC problem is solvable for a given fault estimate $\hat{\boldsymbol{f}}_k$. If this is not the case, then the reference trajectory $\boldsymbol{r}_{[t_1,t_2]}$ must be changed to ensure the feasibility of the MPC problem.

## 6. Illustrative example

The performance of the proposed approach will be illustrated with a cascade two-tank system portrayed in Fig. 2 (Witczak & Pazera, 2024). Such a system consists of two separated tanks placed one above the other. It is also equipped with two pumps feeding individual tanks. The liquid goes out from these tanks under the effect of gravity, and eventually goes back to the reservoir which is a liquid source for the above pumps. By means of a Taylor-based linearization procedure, the mathematical model of such a system can be represented in the state-space form by matrices:

$$\boldsymbol{A}_c = \begin{bmatrix} \frac{-K_m}{2F_m\sqrt{h_1}} & 0 \\ \frac{K_m}{2F_m\sqrt{h_1}} & \frac{-K_m}{2F_m\sqrt{h_2}} \end{bmatrix}, \quad \boldsymbol{B}_c = \begin{bmatrix} \frac{1}{F_m} & 0 \\ 0 & \frac{1}{F_m} \end{bmatrix}. \tag{41}$$

where $\boldsymbol{x} = [h_1, h_2]^T$ is the state consisting of liquid levels in the respective tanks, $K_m = 0.85$ [m$^2$] is the flow constant and $F_m = 3.6$ [m$^2$] stands for the tank cross-section area. All states are measured, i.e. $\boldsymbol{C}_c = \boldsymbol{I}_{m\times m}$. As a consequence of a linearization around $h_1 = h_2 = 0.4$ [m] and discretization with the sampling time $T_s = 1$ [s], the following numerical matrices were obtained:

$$\boldsymbol{A} = \begin{bmatrix} 0.8297 & 0 \\ 0.1549 & 0.8297 \end{bmatrix}, \quad \boldsymbol{B} = \begin{bmatrix} 0.2534 & 0 \\ 0.0229 & 0.2534 \end{bmatrix}. \tag{42}$$

Additionally, a complete description of (14)–(15) and (18)–(20) is obtained with $\boldsymbol{H} = \boldsymbol{C}$, $\boldsymbol{W} = \mathrm{diag}(0.1, 0.1)$ and $\boldsymbol{V} = \mathrm{diag}(0.01, 0.01)$. Moreover, the initial condition of (14)–(15) is set to $\boldsymbol{x}_0 = \begin{bmatrix} 0.1, & 0.1 \end{bmatrix}^T$ while the one of (18)–(20) is $\boldsymbol{x}_{r,k} = \begin{bmatrix} 0, & 0 \end{bmatrix}^T$. Finally, the initial state estimate is considered $\hat{\boldsymbol{x}}_0 = \begin{bmatrix} 0.01, & 0.01 \end{bmatrix}^T$. The vectors $\boldsymbol{w}_k$ and $\boldsymbol{v}_k$ are generated according to the truncated normal distribution with expectation equal to 0, standard deviation $\sigma_w = 0.0577$ and $\sigma_v = 0.1030$ and the truncation level equal to $4 \cdot 10^{-4}$ and $2 \cdot 10^{-4}$, respectively.

**Table 1**
Fault scenarios performed during the experiment.

| Scenario | $\gamma_1$ | $\gamma_2$ |
|---|---|---|
| F-Sc-1 | 0 | 0 |
| F-Sc-2 | −0.2 | 0 |
| F-Sc-3 | −0.5 | 0 |
| F-Sc-4 | −0.9 | 0 |
| F-Sc-5 | 0 | −0.2 |
| F-Sc-6 | 0 | −0.5 |
| F-Sc-7 | 0 | −0.9 |
| F-Sc-8 | −0.4 | −0.6 |
| F-Sc-9 | −0.3 | from 0 to −0.4 |

To verify the proposed approach in the context of fault estimation and fault-tolerant control, eight fault scenarios have been investigated. The actuator fault signals were generated with $f_{i,k} = \gamma_i u_{i,k}$, $i = 1, \ldots, 2$ with actuator performance loss parameters $\gamma_i$ defined in Table 1. Note that $\gamma_i = 0$ indicates that the $i$th actuator is fault-free whilst $\gamma_i = -1$ stands for the complete loss of the $i$th actuator. In scenarios 1–8, the fault occurrence time was set to 40 [s] and 60 [s] for the first and second actuator, respectively. This implies that after 60 [s] both faults appear simultaneously. The fault scenario F-Sc-9 contains both, constant and the time-varying actuator fault. Such a scenario presents a developing fault for the second actuator which changing its behaviour from 40 [s] to 80 [s] by increasing its magnitude to 40% in the time interval equal to 40 [s] from 40 to 80 [s]. The exemplary actuator fault $\boldsymbol{f}_{a,k}$ and its estimate $\hat{\boldsymbol{f}}_{a,k}$ for the F-Sc-9 is presented in Fig. 3. It clearly shows the efficiency of the proposed FTC including fault estimation in both, suddenly changed fault signals as well as slowly developing ones. The FTC ultimate goal is to keep the liquid level at 0.5 [m] and 0.6 [m] for the first and second tank, respectively. However, before proceeding to assess the proposed FTC scheme, the behaviour of the proposed estimator with respect to convergence parameter $\alpha_e \in (0, 1)$ is illustrated. For that purpose, two extreme values $\alpha_e = 0.1$ and $\alpha_e = 0.99$ are used. The difference in the obtained results can be easily observed in Figs. 4–5. The estimator's responses, more specifically, the fault estimates for both actuators are shown in these figures. The actual faults, represented by red solid lines are displayed as abrupt value changes that happen 40 and 60 s after the commencement, which is in keeping with fault scenario F-Sc-8 in Table 1. To examine the efficacy of the suggested estimation procedure, two $\alpha_e$ values were selected: $\alpha_e = 0.1$ and $\alpha_e = 0.99$. The fault estimation produced satisfactory results in both circumstances. For both actuators, the estimates (shown as black solid lines) closely resemble the real defects, demonstrating the estimating algorithm's great precision. As it can be seen, for $\alpha_e = 0.99$, the speed of convergence of the estimate to the real value of the faults is significantly increased compared to what is obtained using $\alpha_e = 0.1$. Nevertheless, the technique can be adjusted to speed up convergence by setting the parameter $\alpha_e$. Empirical evidence has demonstrated that raising $\alpha_e$ accelerates the convergence of fault estimates, which would enable the FTC to respond more quickly.

Now the performance of the proposed FTC scheme is illustrated. Figs. 6–13 present the response of the system obtained with the proposed approach for the different fault scenarios presented in Table 1. For the sake of comparison, a conventional MPC is employed. For all specified fault scenarios in Table 1, the system's responses using the suggested FTC technique are represented by black solid lines in these figures, whereas the estimations for the states are displayed by green solid lines. The reference signals that the control system is trying to follow are indicated by the blue solid lines. For contrast, the results from a typical MPC technique are shown as red solid lines. The fault-tolerant control approach and its estimator appear to be successfully

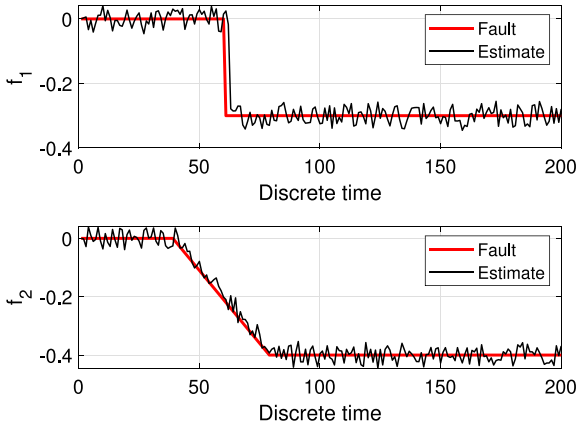


**Fig. 3.** Exemplary faults and their estimates for the F-Sc-9.

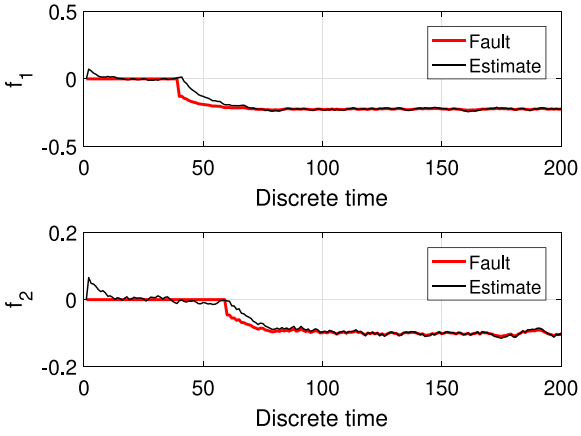


**Fig. 4.** A fault and its estimate obtained with $\alpha_e = 0.1$.

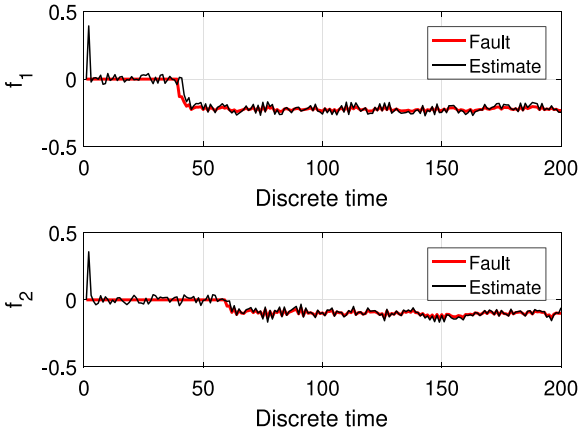


**Fig. 5.** A fault and its estimate obtained with $\alpha_e = 0.99$.

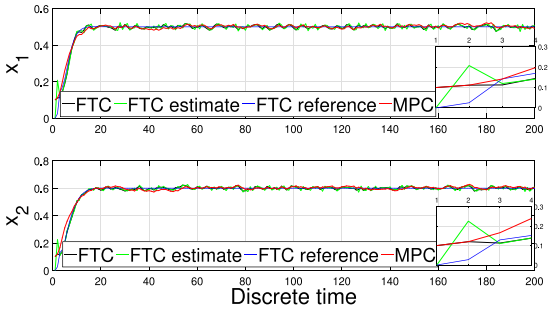


**Fig. 6.** States of the system for fault scenario F-Sc-1.

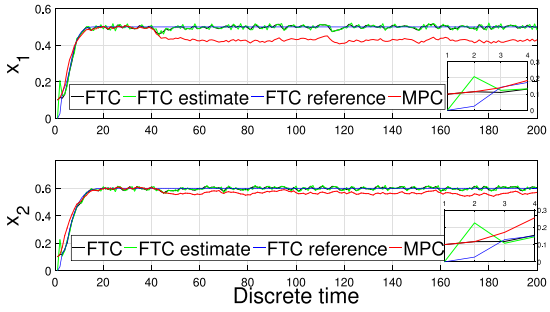


**Fig. 7.** States of the system for fault scenario F-Sc-2.

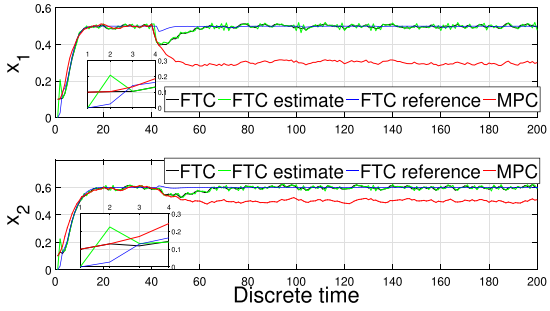


**Fig. 8.** States of the system for fault scenario F-Sc-3.

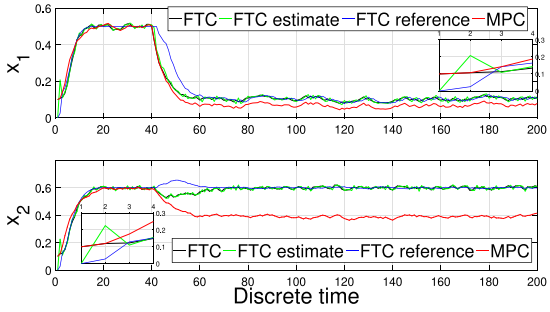


**Fig. 9.** States of the system for fault scenario F-Sc-4.

following the reference signal, as seen by the FTC answers and their estimates closely matching the reference. The data that correspond to scenarios with non-zero fault levels, in particular, show that the results obtained with MPC depart from the reference more than those of the FTC. This supports the claim that the FTC is superior to the traditional MPC. As it can be noticed from the presented results, the proposed approach can tackle the actuator faults with relatively large magnitudes. This, of course, cannot be realized without limits. Indeed, in case of the large actuator fault (F-SC-4) corresponding to the first pump, its compensation is simply impossible as the second pump cannot be used for the necessary control allocation. This unappealing effect is clearly visible in Fig. 9.

Finally, a set of exemplary control signals is presented in Figs. 14–15. They clearly show the effort required for achieving active FTC while satisfying the control bounds.

For the comparison purposes, the proposed approach has been compared to the one presented in Witczak et al. (2013) which similarly uses the nominal control input for the referenced system and the possibly

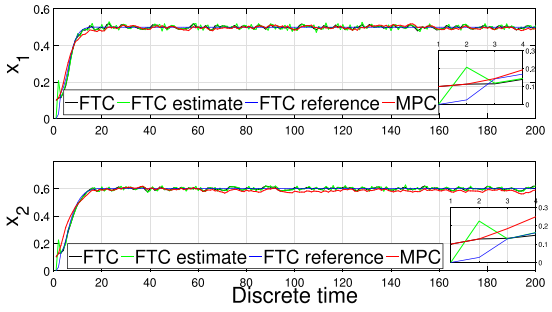


**Fig. 10.** States of the system for fault scenario F-Sc-5.

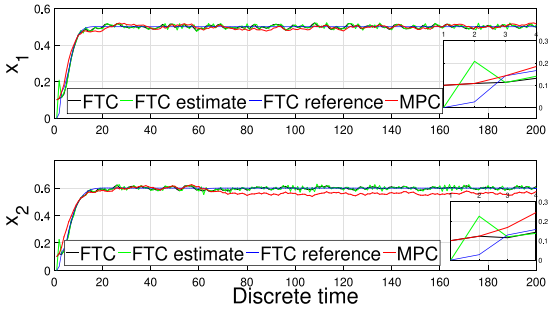


**Fig. 11.** States of the system for fault scenario F-Sc-6.

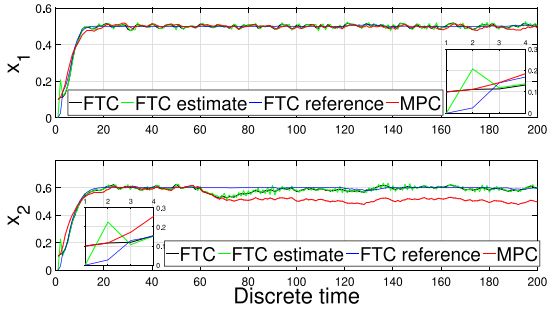


**Fig. 12.** States of the system for fault scenario F-Sc-7.

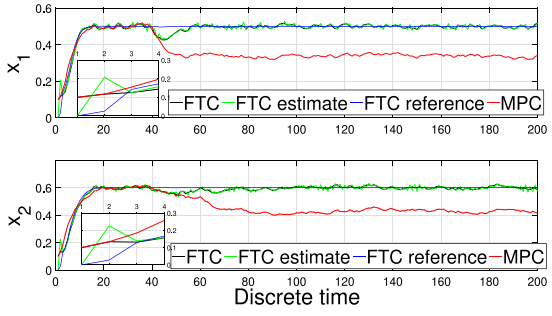


**Fig. 13.** States of the system for fault scenario F-Sc-8.

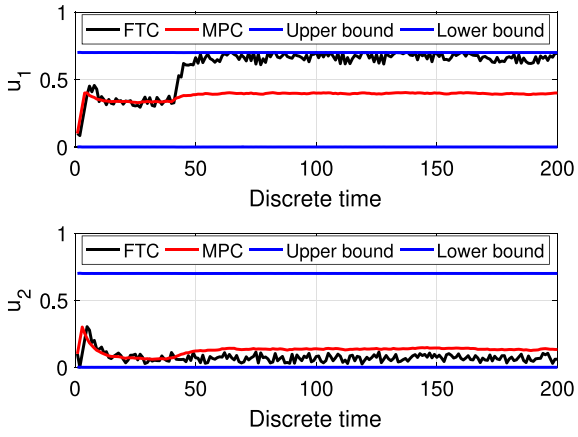


**Fig. 14.** Comparison of the control for fault scenario F-Sc-3.

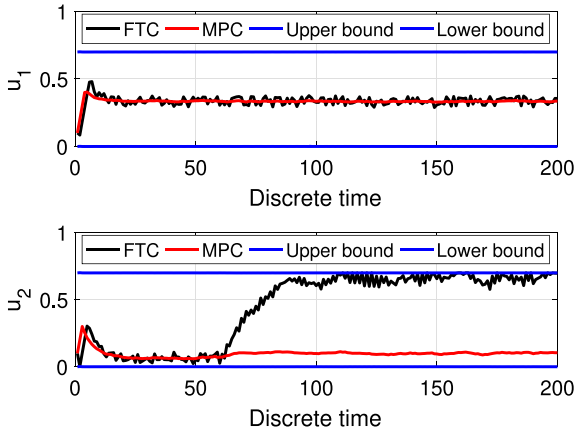


**Fig. 15.** Comparison of the control for fault scenario F-Sc-7.

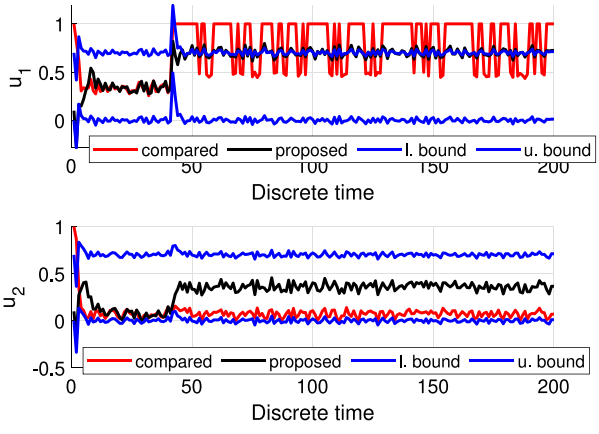


**Fig. 16.** The comparison of the proposed approach with the existing method from Witczak et al. (2013).

faulty one. The comparing approach was also suitably extended to the Lipschitz class nonlinear systems. Fig. 16 shows the comparison of the control input where the black solid line represent the control obtained by the proposed approach while the red line is the control input obtained by the compared one. It is evident that both, proposed and compared approach, in the steady state situation (between 5 and 40 [s]) they have given similar results. This means the control input is nearly the same. The first difference can be observed in the transient phase, when the system tries to reach the reference (between 1 and 10 [s]). In this situation, the proposed approach respects the lower and upper bounds while the compared approach starts with the maximum pump inflow regardless the boundaries and going into saturation. The other situation that shows the difference is when the fault occur (after 40 [s] from the beginning). The proposed approach generates the control input respecting the upper bound, while the compared one generates the control input without taking into account the upper bound going into saturation. It can be easily noticed that the proposed approach gave the control input smooth sliding onto the upper bound during

the fault occurrence while the results obtained with the compared one, this pattern indicates excessive reactivity and lack of smoothness in the control action, which, in practical systems, may result in reduced control performance.

## 7. Conclusions

This paper has proposed design conditions for an integrated FTC strategy for constrained discrete-time linear system affected by bounded external disturbances. The proposed strategy was realized with the quadratic boundedness approach, which makes it possible to formulate the conditions for the integration of fault estimation and FTC. The proposed strategy was developed as an output feedback one, which tracks the desired reference system taking into account faults, disturbances as well as state and input constraints. Finally, the performance of the proposed approach is illustrated with a two-tank system example.

## CRediT authorship contribution statement

**Marcin Witczak:** Writing – original draft, Conceptualization. **Damiano Rotondo:** Writing – original draft. **Marcin Pazera:** Writing – original draft. **Vicenç Puig:** Writing – original draft.

## Declaration of competing interest

The authors declare that they have no known competing financial interests or personal relationships that could have appeared to influence the work reported in this paper.

## Acknowledgements

This work was supported in part by National Science Centre in Poland, grant No. 2020/37/B/ST7/03280.

## References

Alessandri, A., Baglietto, M., & Battistelli, G. (2006). Design of state estimators for uncertain linear systems using quadratic boundedness. *Automatica*, *42*, 497–502.

Braga, M. F., Morais, C. F., Tognetti, E. S., Oliveira, R. C. L. F., & Peres, P. L. D. (2015). Discretization and event triggered digital output feedback control of LPV systems. *Systems & Control Letters*, *86*, 54–65.

Camacho, E., & Bordons, C. (2007). *Model predictive controllers*. Springer.

de Oliveira, M., Bernussou, J., & Geromel, J. (1999). A new discrete-time robust stability condition. *Systems & Control Letters*, *37*(4), 261–265.

Do, M.-H., Koenig, D., & Theilliol, D. (2020). Robust $H_\infty$ proportional-integral observer-based controller for uncertain LPV system. *Journal of the Franklin Institute*, *357*(4), 2099–2130.

Han, J., Liu, X., Wei, X., & Zhu, X. (2023). Reduced-order observer-based finite time fault estimation for switched systems with lager and fast time varying fault. *IEEE Transactions on Circuits and Systems II: Express Briefs*, *71*(1), 350–354.

Han, J., Liu, X., Xie, X., & Wei, X. (2023). Dynamic output feedback fault tolerant control for switched fuzzy systems with fast time varying and unbounded faults. *IEEE Transactions on Fuzzy Systems*, *31*(9), 3185–3196.

Hashemi, M., & Tan, C. (2020). Integrated fault estimation and fault tolerant control for systems with generalized sector input nonlinearity. *Automatica*, *119*, Article 109098.

Karafyllis, I., Ahmed-Ali, T., & Giri, F. (2020). A note on sampled-data observers. *Systems & Control Letters*, *144*, Article 104760.

Kukurowski, N., Mrugalski, M., Pazera, M., & Witczak, M. (2022). Fault-tolerant tracking control for a non-linear twin-rotor system under ellipsoidal bounding. *International Journal of Applied Mathematics and Computer Science*, *32*(2), 171–183.

Lan, J., & Patton, R. (2016a). A new strategy for integration of fault estimation within fault-tolerant control. *Automatica*, *69*, 48–59.

Lan, J., & Patton, R. (2016b). Integrated design of fault-tolerant control for nonlinear systems based on fault estimation and T–S fuzzy modeling. *IEEE Transactions on Fuzzy Systems*, *25*(5), 1141–1154.

Lan, J., & Patton, R. (2021). *Robust integration of model-based fault estimation and fault-tolerant control*. Springer.

Lan, J., & Patton, R. (2022). An iterative strategy for robust integration of fault estimation and fault-tolerant control. *Automatica*, *145*, Article 110556.

Magni, L., Raimondo, D. M., & Scattolini, R. (2006). Regional input-to-state stability for nonlinear model predictive control. *IEEE Transactions on Automatic Control*, *51*(9), 1548–1553.

Montes de Oca, S., Puig, V., Witczak, M., & Dziekan, L. (2012). Fault-tolerant control strategy for actuator faults using LPV techniques: Application to a two degree of freedom helicopter. *International Journal of Applied Mathematics and Computer Science*, *22*(1), 161–171.

Morrison, D., Jacobson, S., Sauppe, J., & Sewell, E. C. (2016). Branch-and-bound algorithms: A survey of recent advances in searching, branching, and pruning. *Discrete Optimization*, *19*, 79–102.

Rotondo, D., Pazera, M., & Witczak, M. (2025). Integrated fault estimation and fault-tolerant control for constrained LPV systems subject to bounded disturbances. *Journal of Process Control*, *145*, Article 103343.

Sala, A., & Ariño, C. (2007). Asymptotically necessary and sufficient conditions for stability and performance in fuzzy control: Applications of Polya's theorem. *Fuzzy Sets and Systems*, *158*(24), 2671–2686.

Witczak, M. (2014). *Fault diagnosis and fault-tolerant control strategies for non-linear systems*: *vol. 266*, Springer.

Witczak, M., Buciakowski, M., & Aubrun, C. (2016). Predictive actuator fault-tolerant control under ellipsoidal bounding. *International Journal of Adaptive Control and Signal Processing*, *30*(2), 375–392.

Witczak, M., Dziekan, L., Puig, V., & Korbicz, J. (2008). Design of a fault-tolerant control scheme for Takagi–Sugeno fuzzy systems. In *16th Mediterranean conference on control and automation* (pp. 280–285). IEEE.

Witczak, M., & Pazera, M. (2024). Towards integrated tracking fault-tolerant control for takagi-sugeno systems. In *2024 IEEE 63rd conference on decision and control* (pp. 2068–2073). IEEE.

Witczak, M., Pazera, M., Majdzik, P., & Matysiak, R. (2024). Development of a guaranteed minimum detectable sensor fault diagnosis scheme. *International Journal of Applied Mathematics and Computer Science*, *34*(3), 409–423.

Witczak, M., Puig, V., & de Oca, S. (2013). A fault-tolerant control strategy for non-linear discrete-time systems: application to the twin-rotor system. *International Journal of Control*, *86*(10), 1788–1799.

Xiao, J., Liu, Y., & An, Y. (2024). Adaptive dynamic event-triggered fault tolerant control for uncertain strict-feedback nonlinear systems. *European Journal of Control*, *79*, Article 101096.